Ring Current Patterns in Annelated Bicyclic Polyenes

Remco W. A. Havenith, Francesca Lugli, Patrick W. Fowler,* and Erich Steiner

School of Chemistry, University of Exeter, Stocker Road, Exeter EX4 4QD, United Kingdom

Received: February 21, 2002; In Final Form: April 19, 2002

Ring-current maps are constructed by Hückel−London theory for the 36 bicyclic systems C_NH_{N-2} derived by formal cross-linking of even [*N*]annulenes ($N \leq 18$). The patterns of circulation are classified according to the length of perimeter and position of the cross-link, described by the five possible combinations of perimeter and constituent ring sizes. The qualitative predictions are tested by ab initio distributed-origin (CTOCD) calculations of the maps for a subset of 15 bicycles in planar geometries. The ab initio calculations confirm the graph-theoretical prediction that the main current follows the Hückel rule: diatropic for "aromatic" $4n + 2$ and paratropic for "antiaromatic" $4n$ π electrons. A perimeter current is found in the ab initio maps, when the bicycle is formed by fusion of two odd rings ($[2l + 1]$, $[2m + 1]$), two *equal* antiaromatic rings ($[4l, 4l]$) or two (not necessarily equal) aromatic rings ($[4l + 2]$, $[4m + 2]$). Orbital analysis shows that these perimeter currents are four-electron diatropic or two-electron paratropic, as in the monocycles. In the other cases, of a $4n + 2$ bicycle formed by fusion of two unequal antiaromatic rings ($[4l, 4m]$) or of a $4n$ bicycle formed from fusion of an antiaromatic and an aromatic ring ($[4l, 4m + 2]$), the current is concentrated in one of the component rings.

Introduction

The distribution of ring currents in unsaturated polycyclic molecules is intrinsic to the understanding of aromaticity in these systems; indeed, in one definition, aromaticity *is* the ability to support an induced diatropic ring current.[1−5] With continuous distributed-gauge methods,[6−9] ring currents can be calculated and mapped from ab initio wave functions, and interpreted in terms of physically based orbital contributions.[10] For monocyclic rings, it has been shown that the diamagnetism of $4n + 2$ systems and the paramagnetism of $4n$ systems arise in the orbital picture from, respectively, four and two frontier electrons.[11]

Here, we extend this description to bicyclic systems, using qualitative ideas to derive systematics of the ring-current patterns in annelated pairs and give rules of thumb that can be checked against ab initio π ring-current maps. Hückel−London theory[12,13] is used to derive ring-current patterns for the 36 even-carbon bicyclic molecules that can be constructed from up to 18 conjugated centers. Ab initio ring-current maps are calculated for a representative subset, using the ipsocentric[10] continuous transformation of current density diamagnetic zero (CTOCD-DZ) method[7,14] in which the current density at any point in space is calculated with that point as origin. The purely graph-theoretical Hückel−London model is seen to provide a useful guide to the essential features of the induced current density in the π systems of bicycles, and it is shown that the overall patterns can be understood in terms of orbital contributions arising from just a few frontier electrons.

A number of these bicyclic systems have been synthesized or have been observed as reactive intermediates, for example, butalene (**15**),[15] bicyclo[3.1.0]hexatriene (**1**),[16] pentalene (**23**),[17] azulene (**3**), benzocyclobutadiene (**31**),[18] heptalene (**26**),[19] and bicyclo[6.2.0]decapentaene (**16**).[20,21] Several systems have also been subjects of theoretical investigations (see, for example, refs 4,17, and 22−29). The reactivity of pentalene (see, for example, ref 17) is in line with its antiaromatic nature (nucleus-independent chemical shift (NICS) of 18.1 ppm[4]). Experimental evidence for the absence or presence of induced ring currents in azulene, benzocyclobutadiene, and bicyclo[6.2.0]decapentaene comes from ^{1}H NMR chemical shieldings. The ^{1}H NMR shifts of the hydrogen atoms of azulene (for which NICS is −19.7 (5-ring) and −7.0 (7-ring) ppm[4]) are all in the "aromatic" range (7.3−8.5 ppm),[30−32] whereas the shifts of the six-membered-ring protons (δ 6.26 and 5.78) and of the four-membered-ring protons (δ 6.36) of benzocyclobutadiene have been taken to indicate nonaromatic nature,[18] though computed NICS values (−2.5 (6-ring), 22.5 (4-ring) ppm) would indicate an antiaromatic four-membered ring.[4] The chemical shifts of the ring protons of bicyclo[6.2.0]decapentaene (δ 6.35 (8-ring) and 7.47 (4-ring))[21] indicate aromatic character. The ^{1}H NMR chemical shifts of benzocyclooctatetraene (**33**) are 7.13/6.9 ppm for the benzenoid protons but in the range 5.8−6.5 ppm for those attached to the cyclooctatetraene moiety.[33] The ^{1}H chemical shifts of heptalene fall in the range 4−5 ppm.[19] Thus, the experimental data suggest that, depending on the initial size of the monocycle and on the position of the cross-link within it, significantly different ring current patterns may exist in bicyclic molecules.

Nomenclature

We consider fused bicycles in which the total number of conjugated carbon centers is either $N = 4n + 2$ or $N = 4n$. The annelated system is formally constructed by fusion of two monocycles of size L and M, where $N = L + M - 2$, or by introducing a cross-link from atom 1 to atom $L = N - M + 2$ into a parent monocycle of size N. The triple $[N, L, M]$ can be used as a shorthand notation for the molecule, and five distinct cases are possible (Table 1): (a) $N = 4n + 2$ and L and M are both odd; (b) $N = 4n + 2$, L and M are both even, $L = 4l + 2$, and $M = 4m + 2$; (c) $N = 4n + 2$, L and M are both even, L

* To whom correspondence should be addressed. Fax: +44-1392-263434. E-mail: P.W.Fowler@exeter.ac.uk.

10.1021/jp0204962 CCC: $22.00
Published on Web 05/17/2002

TABLE 1: Hückel−London Currents in the [*N, L, M*] Bicyclic Systems in Units of the Benzene Ring Current[a]

[*N, L, M*]	$j_L/j_{benzene}$	$j_M/j_{benzene}$	$j_L - j_M$
	Case a		
[*6, 3, 5*] (**1**)	0.798	0.721	0.077
[*10, 3, 9*] (**2**)	1.383	1.216	0.167
[*10, 5, 7*] (**3**)	1.150	1.069	0.081
[*14, 3, 13*] (**4**)	1.956	1.742	0.214
[*14, 5, 11*] (**5**)	1.690	1.485	0.205
[*14, 7, 9*] (**6**)	1.483	1.404	0.079
[*18, 3, 17*] (**7**)	2.522	2.279	0.243
[*18, 5, 15*] (**8**)	2.251	1.961	0.290
[*18, 7, 13*] (**9**)	1.994	1.781	0.213
[*18, 9, 11*] (**10**)	1.812	1.735	0.077
	Case b		
[*10, 6, 6*] (**11**)	1.093	1.093	0.000
[*14, 6, 10*] (**12**)	1.349	1.593	−0.244
[*18, 6, 14*] (**13**)	1.635	2.138	−0.503
[*18, 10, 10*] (**14**)	1.764	1.764	0.000
	Case c		
[*6, 4, 4*] (**15**)	0.717	0.717	0.000
[*10, 4, 8*] (**16**)	2.376	0.359	2.017
[*14, 4, 12*] (**17**)	4.252	0.233	4.019
[*14, 8, 8*] (**18**)	1.422	1.422	0.000
[*18, 4, 16*] (**19**)	6.236	0.168	6.068
[*18, 8, 12*] (**20**)	2.818	0.994	1.824
	Case d		
[*4, 3, 3*] (**21**)	−1.136	−1.136	0.000
[*8, 3, 7*] (**22**)	−2.739	−2.512	−0.227
[*8, 5, 5*] (**23**)	−2.137	−2.137	0.000
[*12, 3, 11*] (**24**)	−4.398	−4.083	−0.315
[*12, 5, 9*] (**25**)	−3.414	−3.190	−0.224
[*12, 7, 7*] (**26**)	−2.980	−2.980	0.000
[*16, 3, 15*] (**27**)	−6.060	−5.698	−0.362
[*16, 5, 13*] (**28**)	−4.927	−4.552	−0.375
[*16, 7, 11*] (**29**)	−4.144	−3.916	−0.228
[*16, 9, 9*] (**30**)	−3.789	−3.789	0.000
	Case e		
[*8, 4, 6*] (**31**)	−3.436	−0.449	−2.987
[*12, 4, 10*] (**32**)	−5.150	−0.276	−4.874
[*12, 6, 8*] (**33**)	−1.480	−5.112	3.632
[*16, 4, 14*] (**34**)	−7.068	−0.193	−6.875
[*16, 6, 12*] (**35**)	−2.601	−7.152	4.551
[*16, 8, 10*] (**36**)	−6.097	−1.061	−5.036

[a] j_L (j_M) is the ring current in the ring of size L (M). A positive value corresponds to diamagnetic circulation, a negative value to paramagnetic circulation, and the difference $j_L - j_M$ is the net current in the common bond.

$= 4l$, and $M = 4m$; (d) $N = 4n$ and L and M are both odd; (e) $N = 4n$, L and M are both even, $L = 4l$, and $M = 4m + 2$, where l, m, and n are integers.

Methods

The ring-current concept is most useful for planar systems, in which rigorous separation of σ and π symmetries is a consequence of symmetry; in planar conjugated hydrocarbons, it is the π electrons that give rise to the ring current, the σ structure typically providing a uniform background of localized circulations.[34] Bicycles containing large rings may not in fact have planar equilibrium structures, but it is possible to enforce planarity even in these cases by the use of suitable clamping groups.[35−38] Previous studies of the effects of clamping on benzene[39] and cyclooctatetraene[40] indicate that the nature of the central current is not thereby changed, provided that the clamping groups are saturated. Thus, the benzene ring current in tris(bicyclo[2.1.1]hexano)benzene remains characteristically diatropic, and the cyclooctatetraene current in tetrakis(bicyclo-[2.1.1]hexeno)cyclooctatetraene remains strongly paratropic. All molecules in the present study are treated as planar, enforcing this condition where necessary. Their computed current-density maps are therefore expected to be good approximations to those for appropriate chemically clamped bicyclic structures, and those for the bare bicycle itself, when the molecule is naturally planar.

Calculations were performed at two levels. First, in a general survey, ring currents were obtained with the Hückel−London[12,13] approach in which all bicycles were modeled with a planar equilateral geometry, taking a C−C bond length of 1.4 Å as a notional benzene value. Systems **1**−**36** (Table 1) were treated in this way. The strength of the currents in the two cycles in this table is expressed in units of the benzene ring current.

For the ab initio treatment, geometries of **2**, **3**, **11**−**13**, **15**−**18**, **20**, **22**, **23**, and **31**−**33** were optimized under the constraint of planarity at the RHF/6-31G** level using GAMESS-UK.[41] Systems **2**, **3**, **11**, **15**, **22**, **23**, and **31** are planar: Hessian calculations in these cases confirm that the planar structure occupies a minimum on the potential energy surface. Diagonalization of the Hessian matrix for the others revealed in each case at least one mode with an imaginary frequency, corresponding to a stabilizing out-of-plane distortion coordinate, and imposition of planarity is therefore a real constraint in these cases. Three systems are found to have less than the maximum possible "topological" symmetry when optimized in the plane. In their planar equilibrium geometries, pentalene (**23**) adopts C_{2h} and azulene (**3**) C_s symmetry, the latter being an artifact of the use of an uncorrelated wave function.[23] For octalene (**18**), the planar conformer of lowest energy has C_{2v} symmetry and is a stationary point with two imaginary frequencies.

The magnetic properties of the planar forms of 15 molecules were computed using the continuous transformation of current density (CTOCD) method[7,14] at the coupled Hartree−Fock level of theory with the SYSMO program[42] in the 6-31G** basis set. Current-density maps were plotted using CTOCD-DZ, and nucleus-independent chemical shifts (NICS)[4] at geometrically defined ring centers were calculated using the PZ2 variant of the method.[9] Current densities induced by a unit perpendicular magnetic field were plotted in a plane $1a_0$ above that of the rings.

In the ipsocentric CTOCD-DZ formulation, the first-order wave function describing response to a magnetic field **B** can be written in an uncoupled approximation as a sum over states,[10]

$$\psi_n^{(1)}(\mathbf{r}) = -\frac{1}{2}\sum_{p>N/2}\psi_p\frac{\langle\psi_p|l|\psi_n\rangle}{\epsilon_p-\epsilon_n}\cdot\mathbf{B} + \frac{1}{2}\mathbf{d}\times\sum_{p>N/2}\psi_p\frac{\langle\psi_p|p|\psi_n\rangle}{\epsilon_p-\epsilon_n}\cdot\mathbf{B}$$

where ψ_n is an unperturbed orbital of energy ϵ_n, and $\psi_n^{(1)}$ is the response of ψ_n to the applied field **B**. In this expression, the sums run over virtual excitations via *rotationally* or *translationally* allowed transitions to unoccupied states ψ_p at energies ϵ_p. For perpendicular fields, the relevant transition operators are the angular momentum about the field direction, l_z, and the linear momentum in the molecular plane, p_x and p_y. The parameter **d** is a displacement with respect to a molecular origin and is to be set equal to the position **r** after the differentiation step in the evaluation of the contribution of ψ_n to the current density.[10]

The sum-over-states form of the expression for $\psi_n^{(1)}$ implies that, other things being equal, the observed current density will be dominated by frontier-orbital contributions; in fact, in the simplest monocyclic π systems, as noted earlier, only the HOMO electrons contribute significantly. Perturbation and

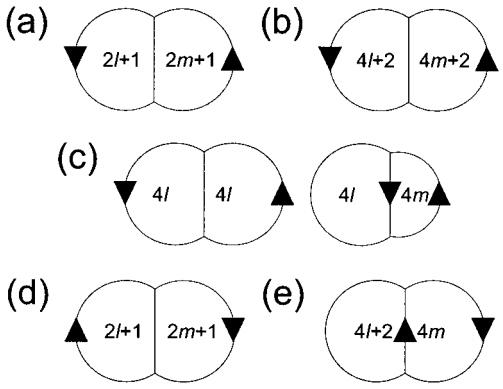

Figure 1. Schematic representation of the bond currents in the five types (a−e) of bicyclic systems created by cross-linking an even annulene. The diagrams show a summary of the general trends in the currents obtained by application of the Hückel−London model for equilateral planar geometries.

SCHEME 1: Ring and Bond Currents in Fused Ring Systems

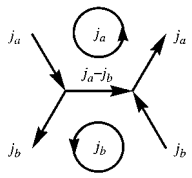

symmetry arguments can be used to rationalize orbital contributions in the bicyclic systems.

Results and Discussion

Hückel−London Currents. The Hückel−London ring currents calculated for the equilateral model geometries of **1**−**36** are summarized in Table 1 and schematically drawn in Figure 1. Diatropic (paratropic) circulations are represented by positive (negative) numbers in Table 1 and shown as anticlockwise (clockwise) in Figure 1. Because the only currents allowed in this model are those flowing along bonds, Kirchhoff's first law applies, and current flowing into any one vertex (carbon site) must flow out again. For bicycles, therefore, the Hückel−London pattern can be expressed as the sum of notional ring-currents j_L and j_M in each subcycle; the current in the common bond is their superposition (Scheme 1). In particular, when j_L and j_M currents are equal and have the same sense, the current in the annelation bond is exactly zero. Inspection of Table 1 reveals several general trends in the Hückel−London currents, which are summarized in Figure 1. The main result is that the sense of the ring current along the perimeter of the system [*N*, *L*, *M*] depends only on *N*, the size of the parent monocycle: if $N = 4n + 2$, as in cases a−c, the current is diatropic, and if $N = 4n$, as in cases d−e, it is paratropic. The perturbation introduced by the cross-linking is evidently not strong enough to reverse the monocycle current. At a more detailed level, the patterns also depend on *L* and *M*, the sizes of the constituent annelated rings, and it is seen that (1) if *L* and *M* are equal the current in the common bond vanishes by symmetry, (2) if *L* and *M* are both odd but unequal the current in the common bond, though nonzero, is negligible in comparison with that on the perimeter, (3) when an $N = 4n + 2$ system is formed by fusion of "aromatic" $L = 4l + 2$ and $M = 4m + 2$ rings the current in the common bond is also negligible, (4) when an $N = 4n + 2$ system is formed by annelation of unequal "antiaromatic" $L = 4l$ and $M = 4m$ rings the strong current in the common bond corresponds to a *diatropic* flow in the smaller ring, and (5) when an $N = 4n$ system is formed by annelation of an "aromatic" $L = 4l + 2$ and an "antiaromatic" $M = 4m$ ring the strong current in the common bond corresponds to paratropic flow in the $4m$ ring.

These observations can be understood in terms of the changes in frontier molecular orbitals and energies induced by cross-linking. First, consider an "aromatic" parent monocycle with $N = 4n + 2$. Initially, HOMO and LUMO are double degenerate and separated by a significant gap. On cross-linking, both pairs split and the HOMO−LUMO gap becomes smaller. In cases a [$4n + 2$, $2l + 1$, $2m + 1$] and b [$4n + 2$, $4l + 2$, $4m + 2$], the splitting and the reduction in gap are small and the ring currents resemble those of the initial monocycle. In case c [$4n + 2$, $4l$, $4m$], in which the constituent rings are both "antiaromatic" cycles, the splitting is substantial and the HOMO−LUMO gap becomes very small, indicating considerable changes in the molecular orbitals; in fact, the current diverts through the common bond in this case, leading to the observed diatropic flow in the smaller component ring.

Now consider an "antiaromatic" parent monocycle with $N = 4n$. In cases d [$4n$, $2l + 1$, $2m + 1$] and e [$4n$, $4l + 2$, $4m$], in which a cross-link is formed in an initial $N = 4n$ monocycle, the half-full degenerate HOMO of the parent splits into the filled HOMO and empty LUMO of the bicycle. In analogy to the distortion of an antiaromatic monocycle from D_{4nh} to D_{2nh} symmetry, cross-linking produces a closed-shell system with a small gap across which a *rotational* (paratropic) transition is allowed.[11] With the symmetry breaking introduced by the cross-linking, other occupied → unoccupied transitions become allowed and can introduce further diamagnetic contributions. The ideas derived from these qualitative Hückel−London calculations can be tested by a consideration of the ab initio current density maps.

Ab Initio Ring Current Maps. The π current-density maps, together with maps of the dominant orbital contributions[10] to the π current for a selection of 15 species from Table 1, are shown in Figures 2 and 3. At least two examples of each case a−e are treated. There is an evident similarity between the Hückel−London and ab initio maps. For all but two of the molecules included in the ab initio subset (the exceptions are **18** and **20**), large currents obtained by the Hückel−London calculation correspond to the main flow in the ab initio computed π current density. Thus, Hückel−London theory correctly predicts the strong diatropic perimeter currents of **2**, **3**, **11**−**13**, and **15**, the strong paratropic perimeter currents of **22** and **23**, the local diatropic currents in the four/eight-membered rings of **16**, **17**, and **20**, and the local paratropic currents in the $4n$ rings of **31**−**33**.

Hückel−London theory fails in detail for the three examples of case c [$4n + 2$, $4l$, $4m$], in which fusion of two unequal "antiaromatic" rings results in a $4n + 2$ system. While Hückel−London theory predicts a diatropic perimeter with the weaker current in the larger ring, the ab initio results show localized (**16**), nonuniform paratropic (**17**), or strong paratropic (**20**) circulation in that larger ring. The Hückel−London model also overestimates the diatropic current of the planarized 14-membered ring in **13** and fails to reproduce the diatropicity of the weaker circulations in the $4n + 2$ rings of case e (**31**−**33**).

The failure of the simplest Hückel−London model for **18** is more apparent than real; if **18** is optimized in full D_{2h} symmetry, the ab initio current density map shows an intense diatropic perimeter circulation, exactly as expected from the graph-theoretical model. However, when the molecule is allowed to

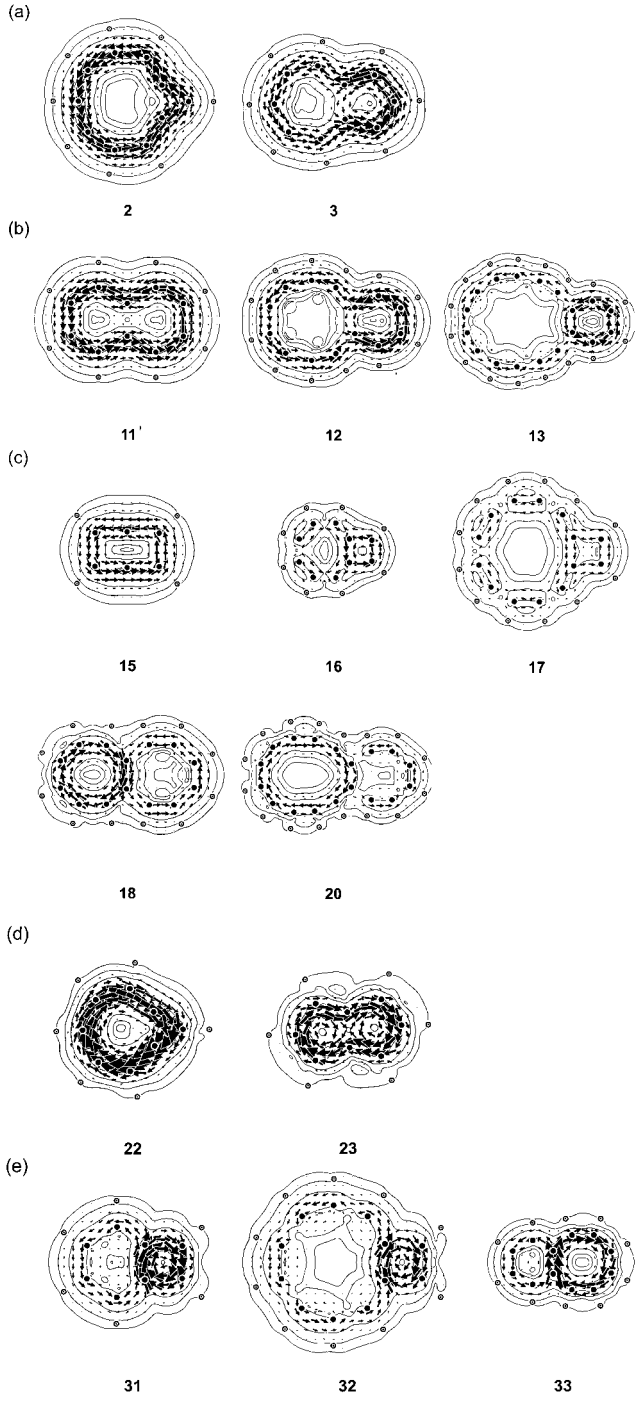

Figure 2. Maps of π current density calculated in the CTOCD-DZ approach for selected molecules optimized at the RHF/6-31G** level with planar constraints. Plotting conventions are as follows:[10] the projection of the current density by unit magnetic field perpendicular to the molecular plane is plotted in the plane $1a_0$ above the molecule with diamagnetic circulation shown as anticlockwise.

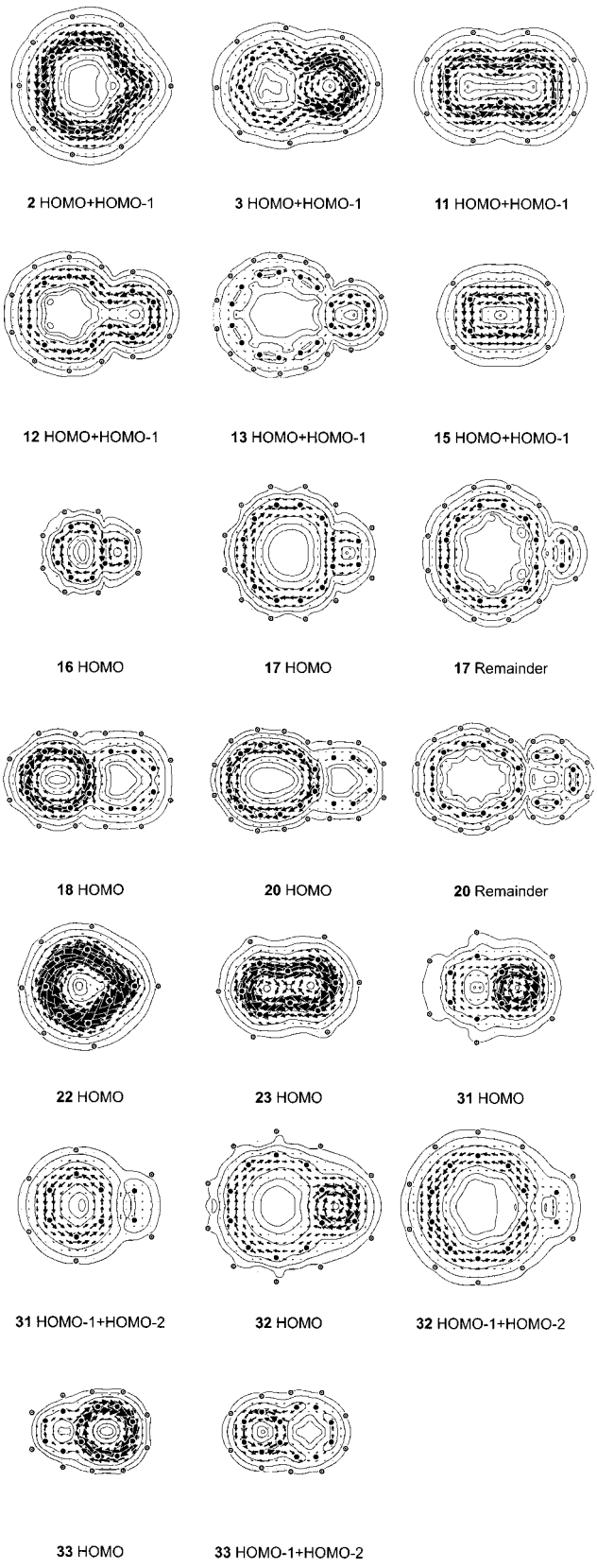

Figure 3. Orbital contributions to the π current density maps of Figure 2. Only the dominant contributions, labeled by orbital and calculated according to the ipsocentric partition (eq 1), are shown. The plotting conventions are the same as those in Figure 2.

distort to C_{2v} symmetry, the ab initio map takes on the appearance of a typical 4*l*, 4*m* bicycle made up of unequal antiaromatic rings. In fact, this distortion is itself predictable within the Hückel model from the value of the largest bond-polarizability eigenvalue, $\lambda_{max} = 1.948\ \beta^{-1}$, which exceeds the threshold for distortion.[43,44] The $D_{2h} \rightarrow C_{2h}$ distortion of pentalene (**23**) is predictable from the same model.[43]

Despite these few discrepancies, most of the observations 1−5 derived from the Hückel−London calculations remain true for the ab initio maps: (1) When *L* and *M* are equal, the vanishing current in the common bond predicted by Hückel−London theory is replaced by a region of negligible current density in the D_{2h}-symmetric systems (**11** and **15**) and a stagnation point

in C_{2h}-distorted pentalene (**23**). (2) The common-bond current for odd−odd systems [$4n + 2$, $2l + 1$, $2m + 1$] remains small in the ab initio maps. (3) The common bond supports a larger current than predicted in "aromatic−aromatic" bicyclic systems [$4n + 2$, $4l + 2$, $4m + 2$], giving a continuous benzenoid current in **12** and **13**, while Hückel−London theory would predict more-or-less complete cancellation. The main feature in observation 4, of strong diatropicity in the smaller ring for [$4n + 2$, $4l$, $4m$], is retained in the ab initio maps, as is the local paratropic flow in the $4m$ ring in [$4n$, $4l + 2$, $4m$] systems described under observation 5.

In view of its tendencies to favor delocalization and to overemphasize charge transfer in unsymmetrical fused bicycles,[45] its inability, as a purely graph-theoretical model, to represent local circulations in bonds, and its neglect of π-distortivity in the crude model with equal weights in all bonds, the overall performance of Hückel−London theory is surprisingly good. The fact that such a simple model approximates the full ab initio maps and is compatible with experimental proton shifts is further confirmation that many of the features of π systems are determined by skeletal topology. For the ab initio maps, it should also be noted that the bicycles with very large constituent rings are more severely constrained when forced to planar geometries, and this in itself may introduce uncertainties into the detail of these ab initio maps. Experience with monocyclic systems suggests that the large paratropic ring currents in some of the constrained bicycles may be moderated in physically clamped versions of the molecules: significant reduction in the central paratropic ring current is predicted to occur when a planar cyclooctatetraene (COT) moiety is clamped in tetrakis(bicyclo[2.1.1]hexeno)cyclooctatetraene,[37,40] for example.

Orbital Contributions. Partition of the total current density into orbital contributions can give further insight into the differences among π systems.[10,11,39,46] In the ipsocentric formulation of these contributions, the diatropic ring current of the $4n + 2$ π-electron monocycle arises from four HOMO electrons, and the paratropic ring current of the $4n$ π-electron monocycle arises from two HOMO electrons. Similar analyses find four magnetically active π-electrons in linear acenes, six in pyracylene, eight in corannulene, and so on.[10] Bicycles belonging to cases a−e can also be classified in this way. Inspection of the orbital contributions to the ab initio maps (Figure 3) show some clear-cut distinctions based on N, L, and M.

Case a [4n + 2, 2l + 1, 2m + 1]. The bicyclic systems derived from the $4n + 2$ monocycles (**2** and **3**) show four-electron diatropicity. Taken together, the contributions of the nondegenerate HOMO and HOMO-1 dominate the total π ring current.

Case b [4n + 2, 4l + 2, 4m + 2]. Where the $4n + 2$ perimeter is built up of two equal "aromatic" rings, the strong diatropic perimeter current is again dominated by the four electrons of the HOMO and HOMO-1. Where the L and M rings are of unequal size, the HOMO and HOMO-1 electrons again give most of the π current density, but contributions from lower-lying orbitals increase in significance for larger systems.

Case c [4n + 2, 4l, 4m]. Where the $4n + 2$ perimeter is built up of two equal "antiaromatic" rings, the strong diatropic perimeter current is again dominated by the four electrons of the HOMO and HOMO-1. Where the L and M rings are of unequal size, or the system is distorted as in **18**, the perimeter current is no longer evident. The HOMO current is paratropic in the larger ring and diatropic in the smaller, and the total contribution of the lower-lying orbitals tends to cancel out the circulation in the larger ring.

TABLE 2: Computed NICS Values for 15 Bicyclic Molecules[a]

[N, L, M] bicycle	NICS(0) L ring	NICS(0) M ring
[*10*, *3*, *9*] (**2**)	−35.7	−11.9
[*10*, *5*, *7*] (**3**)	−16.1 (−19.7)[4]	−8.0 (−7.0)[4]
[*10*, *6*, *6*] (**11**)	−13.0 (−9.9)[4]	−13.0 (−9.9)[4]
[*14*, *6*, *10*] (**12**)	−14.6	−7.0
[*18*, *6*, *14*] (**13**)	−14.6	−3.1
[*6*, *4*, *4*] (**15**)	−2.0	−2.0
[*10*, *4*, *8*] (**16**)	−5.8	1.5
[*14*, *4*, *12*] (**17**)	0.5	0.8
[*14*, *8*, *8*] (**18**)	10.1	−6.6
[*18*, *8*, *12*] (**20**)	−3.1	3.8
[*8*, *3*, *7*] (**22**)	−8.4	18.5
[*8*, *5*, *5*] (**23**)	14.4 (18.1)[24]	14.4 (18.1)[24]
[*8*, *4*, *6*] (**31**)	24.1 (22.5)[4]	−5.6 (−2.5)[4]
[*12*, *4*, *10*] (**32**)	19.2	−2.2
[*12*, *6*, *8*] (**33**)	−9.0	12.4

[a] The quantity NICS(0) is the negative of the absolute shielding at the ring center. For comparison, the NICS(0) value for benzene treated at the same CTOCD-DZ/6-31G**//RHF/6-31G** level is −12.7 ppm.[48]

Case d [4n, 2l + 1, 2m + 1]. Here, the ring current pattern is dominated by the HOMO electrons, and thus, like their parent monocycles, these systems show two-electron paratropicity.

Case e [4n, 4l + 2, 4m]. The partitioning of the total π current shows that these systems are four-electron diatropic and two-electron paratropic, like pyracylene.[10] The contribution of the HOMO is paratropic, concentrating in the $4m$ cycle, and weaker over the perimeter. The combined contribution of the HOMO-1 and HOMO-2 are diatropic in the $4l + 2$ ring, and together the six frontier electrons determine the pattern of counterrotating aromatic and antiaromatic cycles.

Conclusions

Visualization of π current-density maps in bicyclic systems using an ab initio distributed-gauge method shows the surprising extent to which the main predictions of the graph-theoretical Hückel−London model can be trusted. In their planar form, many bicycles exhibit perimeter currents with the sense expected for the isoelectronic monocycle and arising from the same set of frontier orbitals. Though Hückel theory is not always capable of representing the detail of the full ab initio map, the dominant currents are usually well-represented. The CTOCD-DZ approach gives an economical way to obtain fully detailed maps at the Hartree−Fock level, which is sufficient for many π systems of interest.

Another way to assess ring current behavior is through calculations of NICS(0); as Table 2 shows, the values obtained for bicycles are compatible with the maps, subject to known difficulties with the NICS(0) values for three-membered rings,[47] though, as usual, the maps give a more informative picture of the underlying magnetic-field-induced changes in electronic structure.

Acknowledgment. We acknowledge financial support from the European Union TMR Contracts BIOFULLERENES (R.W.A.H.) and USEFULL (F.L.).

References and Notes

(1) Elvidge, J. A.; Jackman, L. M. *J. Chem. Soc.* **1961**, 859.
(2) Smith, M. B.; March, J. *March's Advanced Organic Chemistry. Reactions, Mechanisms and Structure*, 5th. ed.; Wiley-Interscience: New York, 2001.
(3) Pople, J. A. *J. Chem. Phys.* **1956**, *24*, 1111.

(4) Schleyer, P. v. R.; Maerker, C.; Dransfeld, A.; Jiao, H.; van Eikema Hommes, N. J. R. *J. Am. Chem. Soc.* **1996**, *118*, 6317.
(5) Schleyer, P. v. R.; Jiao, H. *Pure Appl. Chem.* **1996**, *68*, 209.
(6) Keith, T. A.; Bader, R. F. W. *J. Chem. Phys.* **1993**, *99*, 3669.
(7) Keith, T. A.; Bader, R. F. W. *Chem. Phys. Lett.* **1993**, *210*, 223.
(8) Zanasi, R.; Lazzeretti, P.; Malagoli, M.; Piccinini, F. *J. Chem. Phys.* **1995**, *102*, 7150.
(9) Zanasi, R. *J. Chem. Phys.* **1996**, *105*, 1460.
(10) Steiner, E.; Fowler, P. W. *J. Phys. Chem. A* **2001**, *105*, 9553.
(11) Steiner, E.; Fowler, P. W. *Chem. Commun.* **2001**, 2220.
(12) London, F. *J. Phys. Radium* **1937**, *8*, 397.
(13) Pasquarello, A.; Schlüter, M.; Haddon, R. C. *Phys. Rev. A* **1993**, *47*, 1783.
(14) Coriani, S.; Lazzeretti, P.; Malagoli, M.; Zanasi, R. *Theor. Chim. Acta* **1994**, *89*, 181.
(15) Breslow, R.; Napierski, J.; Clarke, T. C. *J. Am. Chem. Soc.* **1975**, *97*, 6275.
(16) Marquardt, R.; Sander, W.; Kraka, E. *Angew. Chem., Int. Ed. Engl.* **1996**, *35*, 746.
(17) Bally, T.; Chai, S.; Neuenschwander, M.; Zhu, Z. *J. Am. Chem. Soc.* **1997**, *119*, 1869.
(18) Trahanovsky, W. S.; Fischer, D. R. *J. Am. Chem. Soc.* **1990**, *112*, 4971.
(19) Dauben, H. J., Jr.; Bertelli, D. J. *J. Am. Chem. Soc.* **1961**, *83*, 4659.
(20) Oda, M.; Oikawa, H. *Tetrahedron Lett.* **1980**, *21*, 107.
(21) Kawka, D.; Mues, P.; Vogel, E. *Angew. Chem., Int. Ed. Engl.* **1983**, *22*, 1003.
(22) Ohta, K.; Shima, T. *Chem. Phys. Lett.* **1994**, *217*, 7.
(23) Kozlowski, P.; Rauhut, G.; Pulay, P. *J. Chem. Phys.* **1995**, *103*, 5650.
(24) Zywietz, T. K.; Jiao, H.; Schleyer, P. v. R.; de Meijere, A. *J. Org. Chem.* **1998**, *63*, 3417.
(25) Toyota, A.; Koseki, S.; Shiota, M. *J. Phys. Chem. A* **2000**, *104*, 5343.
(26) Warner, P. M.; Jones, G. B. *J. Am. Chem. Soc.* **2001**, *123*, 10322.
(27) Hess, B. A., Jr. *Eur. J. Org. Chem.* **2001**, 2185.
(28) Winkler, M.; Sander, W. *J. Phys. Chem. A* **2001**, *105*, 10422.
(29) Kraka, E.; Anglada, J.; Hjerpe, A.; Filatov, M.; Cremer, D. *Chem. Phys. Lett.* **2001**, *348*, 115.
(30) Bernstein, H. J.; Schneider, W. G.; Pople, J. A. *Proc. R. Soc. (London), Ser. A* **1956**, *236*, 515.
(31) Hamai, S.; Ikeda, T.; Nakamura, A.; Ikeda, H.; Ueno, A.; Toda, F. *J. Am. Chem. Soc.* **1992**, *114*, 6012.
(32) Selco, J. I.; Brooks, T.; Chang, M.; Trieu, M. T. *J. Org. Chem.* **1994**, *59*, 429.
(33) Elix, J. A.; Sargent, M. V. *J. Am. Chem. Soc.* **1969**, *91*, 4734.
(34) Steiner, E.; Fowler, P. W. *Int. J. Quantum Chem.* **1996**, *60*, 609.
(35) Ermer, O.; Klärner, F.-G.; Wette, M. *J. Am. Chem. Soc.* **1986**, *108*, 4908.
(36) Komatsu, K.; Nishinaga, T.; Aonuma, S.; Hirosawa, C.; Takeuchi, K.; Lindner, H. J.; Richter, J. *Tetrahedron Lett.* **1991**, *32*, 6767.
(37) Matsuura, A.; Komatsu, K. *J. Am. Chem. Soc.* **2001**, *123*, 1768.
(38) Schleyer, P. v. R.; Jiao, H.; Sulzbach, H. M.; Schaeffer, H. F., III *J. Am. Chem. Soc.* **1996**, *118*, 2093.
(39) Fowler, P. W.; Havenith, R. W. A.; Jenneskens, L. W.; Soncini, A.; Steiner, E. *Chem. Commun.* **2001**, 2386.
(40) Fowler, P. W.; Havenith, R. W. A.; Jenneskens, L. W.; Soncini, A.; Steiner, E. *Angew. Chem.*, in press.
(41) Guest, M. F.; van Lenthe, J. H.; Kendrick, J.; Schöffel, K.; Sherwood, P.; Harrison, R. J. *GAMESS-UK*, a package of ab initio programs, with contributions from Amos, R. D.; Buenker, R. J.; van Dam, H. J. J.; Dupuis, M.; Handy, N. C.; Hillier, I. H.; Knowles, P. J.; Bonai-Koutecký, V.; von Niessen, W.; Harrison, R. J.; Rendell, A. P.; Saunders, V. R.; Stone, A. J.; Tozer, D. J.; de Vries, A. H, 2000. It is derived from the original GAMESS code by: Dupuis, M.; Spangler, D.; Wendolowski, J. *NRCC Software Catalog, Vol. 1*, Program No. QG01 (GAMESS), 1980.
(42) Lazzeretti, P.; Zanasi, R. *SYSMO package*; University of Modena: Modena, Italy, 1980; additional routines by E. Steiner and P. W. Fowler.
(43) Binsch, G.; Heilbronner, E.; Murrell, J. N. *Mol. Phys.* **1966**, *11*, 305.
(44) Fowler, P. W.; Rassat, A. *Phys. Chem. Chem. Phys.*, in press.
(45) Streitwieser, A., Jr. *Molecular Orbital Theory for Organic Chemists*, 2nd. ed.; John Wiley & Sons: New York, 1962.
(46) Steiner, E.; Fowler, P. W. *Chem. Phys. Chem.* **2002**, *3*, 114.
(47) Jemmis, E. D.; Subramanian, G.; Kos, A. J.; Schleyer, P. v. R. *J. Am. Chem. Soc.* **1997**, *119*, 9504.
(48) Fowler, P. W.; Steiner, E.; Acocella, A.; Jenneskens, L. W.; Havenith, R. W. A. *J. Chem. Soc., Perkin Trans. 2* **2001**, 1058.